Am. J. Hum. Genet. 76:1008–1022, 2005

Heterozygous Mutations of *OTX2* Cause Severe Ocular Malformations

Nicola K. Ragge,[1,6,8,*] Alison G. Brown,[9,*] Charlotte M. Poloschek,[11] Birgit Lorenz,[11] R. Alex Henderson,[12] Michael P. Clarke,[13] Isabelle Russell-Eggitt,[2] Alistair Fielder,[3] Dianne Gerrelli,[4] Juan Pedro Martinez-Barbera,[4] Piers Ruddle,[4] Jane Hurst,[7] J. Richard O. Collin,[6] Alison Salt,[2,6] Simon T. Cooper,[9] Pamela J. Thompson,[5] Sanjay M. Sisodiya,[5] Kathleen A. Williamson,[10] David R. FitzPatrick,[10] Veronica van Heyningen,[10] and Isabel M. Hanson[9]

[1]Department of Adnexal Surgery, Moorfields Eye Hospital, [2]Great Ormond Street Hospital for Children, [3]Department of Optometry and Visual Science, City University, [4]Neural Development Unit, Institute of Child Health, and [5]Department of Clinical and Experimental Epilepsy, Institute of Neurology, University College London, London; [6]Department of Human Anatomy and Genetics, University of Oxford, and [7]Clinical Genetics Department, Oxford Radcliffe Hospitals NHS Trust, Oxford, United Kingdom; [8]Birmingham Children's Hospital NHS Trust, Diana Princess of Wales Children's Hospital, Birmingham, United Kingdom; [9]University of Edinburgh, School of Molecular and Clinical Medicine, and [10]Medical Research Council Human Genetics Unit, Edinburgh; [11]University of Regensburg, Department of Pediatric Ophthalmology and Ophthalmogenetics, Regensburg, Germany; and [12]Institute of Human Genetics and [13]Claremont Wing Eye Department, Royal Victoria Infirmary, Newcastle upon Tyne, United Kingdom

Major malformations of the human eye, including microphthalmia and anophthalmia, are examples of phenotypes that recur in families yet often show no clear Mendelian inheritance pattern. Defining loci by mapping is therefore rarely feasible. Using a candidate-gene approach, we have identified heterozygous coding-region changes in the homeobox gene *OTX2* in eight families with ocular malformations. The expression pattern of *OTX2* in human embryos is consistent with the eye phenotypes observed in the patients, which range from bilateral anophthalmia to retinal defects resembling Leber congenital amaurosis and pigmentary retinopathy. Magnetic resonance imaging scans revealed defects of the optic nerve, optic chiasm, and, in some cases, brain. In two families, the mutations appear to have occurred de novo in severely affected offspring, and, in two other families, the mutations have been inherited from a gonosomal mosaic parent. Data from these four families support a simple model in which *OTX2* heterozygous loss-of-function mutations cause ocular malformations. Four additional families display complex inheritance patterns, suggesting that *OTX2* mutations alone may not lead to consistent phenotypes. The high incidence of mosaicism and the reduced penetrance have implications for genetic counseling.

Introduction

Abnormalities in the ocular development program can lead to a variety of major structural defects of the eye that present at birth (Graw 2003). At the severe end of the spectrum are anophthalmia (absence of the eye [MIM 206900]) and extreme microphthalmia (small eye [MIM 309700]), which are likely to result from a variety of developmental pathologies (Morrison et al. 2002). Other common malformations include sclerocornea (MIM 181700); anterior chamber malformations, including aniridia (MIM 106210), colobomata (MIM 120200), and congenital cataracts (MIM 116700); and disorders of early retinal differentiation. Diagnostically useful subclasses within these groups include optic-fissure closure defects (colobomata affecting iris, optic nerve, retina, and choroid) (Morrison et al. 2002), disorders of early retinal differentiation (Leber congenital amaurosis [LCA {MIM 204000}] and Walker-Warburg syndrome [MIM 236670]) (Dobyns et al. 1989), and disorders of lens induction or differentiation (congenital cataract/aphakia [MIM 177075]) (Jamieson et al. 2002). Each of these can be isolated or associated with microphthalmia and/or anophthalmia.

Ocular malformations display a broad range of inheritance patterns. Classic aniridia is almost always caused by *PAX6* (MIM 607108) haploinsufficiency and is transmitted with high penetrance and expressivity (Hanson 2003). In contrast, anophthalmia and severe microphthalmia show some evidence of familial recurrence but usually no clear Mendelian transmission pattern (Morrison et al. 2002). This is likely to be a reflection of several potentially interactive factors: oligogenic causation, gene-environment interactions, and stochastic variation in development. There is increasing recognition that, although non-Mendelian inheritance

Received February 2, 2005; accepted for publication April 1, 2005; electronically published April 21, 2005.

Address for correspondence and reprints: Dr. Veronica van Heyningen, Medical Research Council Human Genetics Unit, Western General Hospital, Edinburgh, EH4 2XU, United Kingdom. E-mail: v.vanheyningen@hgu.mrc.ac.uk

* These two authors contributed equally to this work.

0002-9297/2005/7606-0008$15.00

patterns make gene identification more difficult, they are ultimately very revealing about the complex molecular networks that contribute to normal development (Ming and Muenke 2002; van Heyningen and Yeyati 2004).

Several genes for anophthalmia, microphthalmia, and coloboma (*RAX* [MIM 601881], *CHX10* [MIM 142993], *PAX6, MAF* [MIM 177075], and *SOX2* [MIM 184429]) have been identified by different methods, ranging from the candidate-gene approach to positional identification, often using informative chromosomal rearrangements (Azuma et al. 1999; Ferda-Percin et al. 2000; Jamieson et al. 2002; Fantes et al. 2003; Graw 2003; Voronina et al. 2004). Apart from *SOX2,* which appears to account for ~10% of severe anophthalmias (Fantes et al. 2003; Ragge et al. 2005), none of these can be considered a major causative gene, because each examined cohort revealed mutations in a very small proportion of affected individuals. We decided to search for additional causative mutations, using a candidate-gene approach.

OTX2 (MIM 600037), a bicoid-type homeodomain gene, is a vertebrate ortholog of the *Drosophila* gene *orthodenticle* (*Otd*), which is required for anterior brain, eye, and antenna formation (Finkelstein and Boncinelli 1994) and for regulating the development of photoreceptors and the expression of rhodopsin (Tahayato et al. 2003). Mammals have three *Otx* genes: *Otx1, Otx2,* and the more diverged *Crx,* which is known as "*Otx5*" in lower vertebrates (Germot et al. 2001). All three genes are expressed in the developing eye—*Crx* almost exclusively so. Human *CRX* (MIM 602225) mutations have been reported in retinal degenerations, including cone-rod dystrophy (MIM 120970), late-onset pigmentary retinopathy, and LCA (Freund et al. 1997; Sohocki et al. 1998; Rivolta et al. 2001). Mouse *Otx1* and *Otx2* are expressed in developing neural and sensory structures, including the brain, ear, nose, and eye (Simeone et al. 1993; Martinez-Morales et al. 2001). The spatiotemporally complex expression pattern is reflected in the large flanking region that is occupied by enhancers required for the regulation of *Otx2* expression (Kurokawa et al. 2004*a*, 2004*b*). Ectopic expression studies in *Xenopus* suggest that *Otx2* operates early, interacting with a network of eye-field transcription factors, including *Rx1, Pax6,* and *Six3* (Zuber et al. 2003). During eye morphogenesis, initial expression in the entire optic vesicle becomes restricted to the presumptive retinal pigment epithelium (RPE) (Simeone et al. 1993; Bovolenta et al. 1997; Martinez-Morales et al. 2001), where OTX2 protein interacts with the transcription factor MITF (MIM 156845), leading to the activation of target genes, including tyrosinase (Martinez-Morales et al. 2003). Later, OTX2 is increasingly expressed in neural retinal cells, including postmitotic neuroblasts (Bovolenta et al. 1997; Nishida et al. 2003). Conditional ablation of *Otx2* in neural retina leads to loss of *Crx* expression and failure of photoreceptor development (Nishida et al. 2003).

Homozygous *Otx2*-knockout embryos have gastrulation defects and die at midgestation with severe brain anomalies (Acampora et al. 1995; Ang et al. 1996). Heterozygotes show highly variable phenotypes—ranging from acephaly; through micrognathia, anophthalmia, and microphthalmia; to normal—depending on genetic background (Acampora et al. 1995; Matsuo et al. 1995; Ang et al. 1996). Recurrent interstitial deletions of human chromosome 14q22-q23 have been consistently associated with anophthalmia (Brewer et al. 1998). No definitive analysis of *OTX2* has been reported in these cases, but the gene maps to the 14q22 genomic region and is a strong candidate for mutation studies in anophthalmia and related eye anomalies.

We therefore undertook mutation analysis of the *OTX2* gene. The common 289-aa isoform is transcribed from a 5-kb genomic region encompassing three exons. The protein has a homeodomain and a 192-aa proline-, serine-, and threonine-rich C-terminal region, which contains a highly conserved SIWSPA peptide sequence and a tandemly duplicated OTX tail, all motifs shared with OTX1 (MIM 600036) and CRX (Germot et al. 2001). Unrelated patients ($n = 333$) with a spectrum of ocular malformations were assessed by direct sequencing. Brain magnetic resonance imaging (MRI) data were obtained for two affected individuals and for an unaffected mutation carrier, and older diagnostic images from other patients were reassessed. The *OTX2* expression pattern was studied in early human embryos for comparison with the known mouse pattern.

Material and Methods

Patients and Controls

Patients with ocular malformation spectrum defects ($n = 333$) were recruited, with informed consent and with appropriate ethics review committee approvals. Detailed case histories of individuals with *OTX2* coding-region sequence changes are available in appendix A (online only). Control DNAs ($n = 164$) from apparently healthy adults were anonymized; they matched the patients in ethnicity (apart from patient 7, who was of African origin [see the "Results" section]). We sequenced 94 DNAs in full, and a further 70 partially, over the region of the proline missense mutations.

DNA Preparation

Genomic DNA was prepared from peripheral blood by use of a Nucleon DNA extraction kit (Tepnel Life Sciences). Buccal cell lysates were prepared from mouth-

wash samples by resuspending the cell pellet in 100 μl of 0.05 M NaOH, heating in a boiling water bath for 20 min, and then neutralizing with 12.5 μl of 1 M Tris (pH 7.6).

PCR and Sequencing

The human *OTX2* cDNA (GenBank accession number NM_172337) is encoded by three exons that are located in BAC AL161757 (GenBank) at positions 59950–60217 (exon 1), 61214–6138 (exon 2), and 6322–64868 (exon 3). The cDNA numbering is derived from the human *OTX2* cDNA (GenBank accession number NM_172337). We designed four genomic amplicons to cover the *OTX2* coding region and some flanking intronic sequences in each case: amplicon 1 contained exon 1, amplicon 2 contained exon 2, and overlapping amplicons 3a and 3b covered the coding part of exon 3. PCR primers are shown in table 1. PCRs were performed in 96-well plates. For amplicons 1 and 2, 50 ng genomic DNA was amplified in a volume of 50 μl containing 1 × Qiagen HotStar*Taq* PCR buffer, 1.5 mM $MgSO_4$, 5 μl PCR enhancer buffer (Invitrogen), 0.2 mM dNTPs, 250 nM forward primer, 250 nM reverse primer, and 2 U of HotStar*Taq* polymerase. For amplicons 3a and 3b, the PCR enhancer buffer was omitted and was replaced with 10 μl of Q solution (Qiagen). Thermal cycling was performed using an MJ PTC225 machine. PCR conditions were 1 cycle of 95°C for 15 min; 35 cycles of 94°C for 30 s, 55°C for 30 s, and 72°C for 1 min; and 1 cycle of 72°C for 5 min.

PCR products were run on a 2% agarose gel to ensure adequate yield and to check for the absence of nonspecific products. Unincorporated primers and dNTPs were removed by incubating 5 μl of PCR product with 1 μl of ExoSapIT (exonuclease I and shrimp alkaline phosphatase enzyme mix [USB]) for 45 min at 37°C, followed by 20 min at 80°C to inactivate the enzyme.

Direct Sequencing

Sequencing of PCR products was performed in a 96-well plate format, as described elsewhere (Aijaz et al. 2004), with the use of forward and reverse primers as shown in table 1. Individual sequence traces were inspected using Chromas software (Technelysium). Multiple sequence traces were aligned and compared using the phredPhrap program from the Consed package (see the Laboratory of Phil Green Web site). All changes were verified by performing a second PCR and sequencing reaction on the patient's DNA. Family members were analyzed if samples were available.

RNA In Situ Hybridization

The expression pattern of *OTX2* was investigated by nonradioactive RNA in situ hybridization in human embryos from Carnegie stages (CS) 14–22, which correspond approximately to mouse Theiler stages 18–23 (E11.25–E15.25). Human embryos were obtained from the Medical Research Council/Wellcome Trust Human Developmental Biology Resource, with full ethical approval. Preparation of embryo sections and nonradioactive RNA in situ hybridization was performed as described elsewhere (Lai et al. 2003).

The template for the *OTX2* probe was a 1.1-kb fragment that was PCR amplified from exon 3 with the use of primers hOTX2A (5′-GCG GAT CCA GTG CTC CTG TGT CTA TCT GGA G-3′) and hOTX2D (5′-GCG AAT TCC AGA GGT GGA GTT CAA GGT TGC-3′) and that was cloned into pGEM-3Z. The construct was linearized with *Bam*HI and was transcribed with T7 RNA polymerase to synthesize the digoxygenin-labeled antisense riboprobe.

Table 1

PCR Primers for Amplification of the *OTX2* Coding Region

The table is available in its entirety in the online edition of *The American Journal of Human Genetics*.

MRI Analysis

MRI scanning was approved by the local institutional ethics committees. All patients scanned for the present study provided written informed consent. Patient 5 and his unaffected mother underwent MRI scanning. MRI acquisition parameters were TE = 4.2, TI = 450, TR = 15, NEX = 1, flip angle = 20°, acquisition matrix 256 × 128, and field of view 24 cm; 124 contiguous slices were produced, with voxel dimension 0.9375 mm × 0.9375 mm × 1.5 mm. An equivalent sequence was used for patient 4B. These data were reformatted in multiple planes to allow careful examination of regions of interest. Additionally, signal changes were inspected on T2 and FastFLAIR sequences (T2 and PD sequence: TE1 = 30, TE2 = 120, TR = 2000, NEX = 1, acquisition matrix 256 × 128, field of view 24 cm × 18 cm, and slice thickness 5 mm contiguous; FastFLAIR sequence: TE1 = 152, TE2 = 2200, TR = 10002, NEX = 1, acquisition matrix 256 × 128, field of view 24 cm, and slice thickness 5 mm contiguous). Patient 4B underwent similar high-resolution T1-weighted MRI scanning. For patients 1, 2, and 6, existing MRI data were reviewed. For patient 3A, CT scan data were reviewed.

Psychometric Testing

Patient 5 and his mother underwent standard neuropsychometric testing, omitting any tests requiring visual function. This component of the study was also approved by the local institutional ethics committee and

was undertaken after written informed consent was obtained.

Results

OTX2 *Mutation Analysis*

Of the 333 patients analyzed, 8 showed sequence variation in the *OTX2* coding region. The changes are distributed throughout the ORF (fig. 1). Additional family members were analyzed, if samples were available, for a total of 11 affected individuals in eight families (fig. 1). Detailed case histories of affected individuals are presented in appendix A (online only), and the phenotypes are summarized in table 2. In the course of the study, we uncovered evidence of mosaicism; therefore, when possible, we also analyzed oral epithelial DNA (obtained by mouthwash or buccal scrape).

Patient 1, with bilateral anophthalmia, has a de novo frameshifting insertion (c.635insGC) at codon 155 in exon 3, the A in the SIWSPA motif (figs. 1 and 2 and table 2). Subsequent out-of-frame translation of 22 amino acids is predicted to terminate at a TGA codon, beginning at c.701. Neither the parents nor the unaffected brother carry the mutation (fig. 1). Identical results were obtained with buccal cell DNA from all four individuals.

Patient 2, with bilateral optic-nerve aplasia (MIM 165550) and microphthalmia (fig. 3 and table 2), has a de novo transversion, c.436C→G, in exon 3 (fig. 1). This is predicted to produce an arginine-to-glycine (R89G) change at position 52 of the homeodomain. Neither parent carries the change in lymphocyte DNA (fig. 1).

Patient 3A, with severe bilateral microphthalmia, has an N-terminal domain frameshifting mutation, c.252delC, in codon 27 of exon 1 (figs. 1 and 2 and table 2). Out-of-frame translation is predicted until the first base of a termination codon is encountered at c.320 in exon 2. A fetus (patient 3B [fig. 1]), terminated after ultrasound diagnosis of affected status, also carried the same mutation. The phenotypically normal mother of patients 3A and 3B was found to have the mutation at low levels in blood and buccal DNA before the existence of the affected fetus was revealed. The unaffected father and maternal grandparents do not have the mutation in blood DNA (fig. 1). These data indicate that the mother is a gonosomal (gonadal and somatic) mosaic carrier of the mutation (Edwards 1989).

Siblings 4A and 4B—diagnosed with microphthalmia and severe developmental delay and with LCA, respectively (figs. 2 and 4 and table 2)—carry a transversion, c.708T→A, in exon 3 (fig. 1). The tyrosine-to-termination (TAT→TAA) change at codon 179 is in the C-terminal domain. Their mother (patient 4C) is a gonosomal mosaic for the Y179X mutation (fig. 1). She has a later-onset phenotype resembling pigmentary retinopathy (fig. 4).

Patient 5, with bilateral anophthalmia, has a frameshifting deletion, c.288delCC, in codons 39–40 in exon 2, at the start of the homeodomain (figs. 1 and 2 and table 2). This mutation is predicted to generate a 46-aa nonsense peptide before reaching a TAA termination codon, beginning at c.429 in exon 3. The phenotypically normal mother of this patient has full representation of the same mutation in both lymphocyte and buccal DNA, indicating that she is probably a nonmosaic mutation carrier. The unaffected father, brother, and sister do not carry the mutation (fig. 1).

Patient 6, with bilateral anophthalmia, has the transition c.466C→T in exon 3 (figs. 1 and 2 and table 2). Glutamine (CAA) is substituted by a termination codon (TAA) at the second amino acid of the C-terminal domain (Q99X). The phenotypically normal father shows full expression of the same mutation in his blood DNA, suggesting that he is a constitutive mutation carrier. The unaffected mother does not have the mutation (fig. 1).

Patient 7, with bilateral microphthalmia and left sclerocornea, has the transversion c.568C→A in exon 3 (figs. 1 and 2 and table 2). This results in replacement of proline (CCC) with threonine (ACC) at position 133 (P133T). The patient's phenotypically normal mother and brother have the same change, but the patient's unaffected father and sister do not (fig. 1). Identical results were obtained with DNA from blood and oral epithelium from all five family members. P133 occurs at the end of a highly conserved hexapeptide motif, SGQFTP, in the C-terminal domain of vertebrate Otx2, Otx1, and Crx proteins (Germot et al. 2001).

Patient 8, with unilateral anophthalmia, has the transversion c.571C→G in exon 3 (figs. 1 and 2 and table 2). This replaces proline (CCC) with alanine (GCC) at amino acid position 134 (P134A). The patient's similarly affected mother does not have this variant in blood or oral epithelium. The father was not available for analysis. The patient's unaffected maternal grandmother and maternal great-grandmother do not have the change, nor does a maternal half brother (fig. 1).

Ninety-four control individuals (188 chromosomes) were examined by direct sequencing for the presence of all the coding-region variants. An additional 70 individuals were sequenced for the region containing prolines 133 and 134. None of the changes was observed in the controls. Ethnic matching was not feasible for family 7, who are of African origin, and therefore no conclusion can be drawn about the frequency of this change in the population from which patient 7 comes.

We detected three SNPs during the course of the present study. All were located in noncoding regions: two newly reported sites (submitted to NCBI dbSNP) in the first intron, 268+12 C/T (dbSNP accession number

Table 2

Summary of Clinical Features

Feature	Patient								
	1	2	3A	4A	4B	5	6	7	8
Sex	Male	Male	Female	Female	Male	Male	Male	Female	Male
DNA mutation	c.635insGC	c.436C→G	c.252delC	c.708T→A	c.708T→A	c.288delCC	c.466C→T	c.568C→A	c.571C→G
Protein mutation	FS	R89G	FS	Y179X	Y179X	FS	Q99X	P133T	P134A
Exon with mutation	3	3	1	3	3	2	3	3	3
De novo mutation	Y	Y	N	N	N	N	N	N	Y?
Maternal age at patient's birth (years)	21		23	18	26	31	22	23	22
Paternal age at patient's birth (years)	22		24			39	25	29	21
Maternal genotype	WT	WT	mos c.252delC	(Patient 4C[a]) mos c.708T→A (Y179X)	(Patient 4C[a]) mos c.708T→A (Y179X)	c.288delCC	WT	c.568C→A	WT
Paternal genotype	WT	WT	WT			WT	c.466C→T	WT	
Maternal phenotype	Hypopigmented macula/fundus	Normal	Normal	(Patient 4C[a]) pigmentary retinopathy	(Patient 4C[a]) pigmentary retinopathy	Normal	Normal	Normal	Left anophthalmia
Paternal phenotype	No reported visual difficulties	Normal	Normal	Normal	Normal	Normal	Normal	Normal	Normal
Birth weight (g)	2,884	2,837	2,700	3,108		4,256		5,000	3,402
Birth OFC[b] (cm)		33		42	41	3rd–10th percentile			39
Gestation (wk)	38	38	40	40	39	42	38	42	42
Age at most recent assessment	4 years	6.3 years	12 years, 11 mo	33 years	25 years	24 years	11 years, 1 mo	4 years	9 years
Height (age)	25th–50th percentile (2.5 years)	10th–25th percentile, 113 cm (6.3 years)		149 cm	160 cm (25 years)	3rd percentile (24 years)		75th percentile, 113.5 cm	10th percentile, 78 cm (1 year)
Weight (age)	<3rd percentile (2.5 years)	25th–50th percentile, 21.4 kg (6.3 years)		65 kg	83.5 kg (25 years)	73.4 kg		97th percentile, 25.5 kg	25th percentile, 10.5 kg (1 year)
Head OFC[b] (age)	<.4th percentile, 48 cm (4 years)	46.2 cm (1 year, 1 mo)		53 cm (33 years)	54.3 cm (25 years)	3rd–10th percentile		97th percentile, 53.4 cm	44.6 cm (1 year)
Vision	None	None	None	None	6/60	None	None	None	R: 6/9.5
Clinical anophthalmia	Right	No	No	No	No	Bilateral	Bilateral	No	Left
Orbital cystic remnants	R: no; L: NA	No	No	NA	NA	None	Bilateral	NA	No
Microphthalmia	Left	Bilateral	Bilateral, severe	Bilateral	Bilateral, mild	NA	NA	Bilateral	NA
Axial length (mm)	L: 12				L: 20; R: 20	R: 4.4; L: 4.9		L: 12–14	R: 20; L: 14
Corneal diameter (mm)	R: NA; L: 8	R: 6.5; L: 7.5	NA	R: 4; L: 4	R: 11; L: 11	NA	NA	R: 3	L: NA; R: ?
Coloboma	Left chorioretinal	No	NA	Bilateral? (report at 1 year, 7 mo)	No	NA	NA	No	No
Anterior segment dysgenesis	No		NA	Corectopia with bilateral iris colobomata	Bilateral anterior synechiae	NA	NA	Left sclerocornea	No

Cataracts	No	Bilateral tunica vasculosa lentis, clear lenses neonatally	NA	L: cataract, later onset	No	NA	NA	R: phthisical after postcataract extraction	Yes
Persistent pupillary membrane	Left	Bilateral	NA		No	NA	NA		No
Retinal vessels		Not visible	NA		Thin	NA	NA		Normal
Optic disk	At edge of coloboma	Abnormal	NA		Atrophic	NA	NA		Normal
Macula	NA		NA		Atrophic	NA	NA		Normal
Retinal pigment	NA		NA		Clumps midperiphery	NA	NA		
Optic nerve on MRI	R: absent; L: small	No	Reduced (CT scan)	No MRI	Yes	Very small, especially intracranially	No	No MRI	No MRI
Optic chiasm on MRI	Thin	No		No MRI	Yes	Very thin	No	No MRI	No MRI
ERG		Very small	NA		Absent	NA	NA		
Visual evoked potential		Absent	NA			NA	NA		
Learning disability	Severe	None	No	Severe	Mild	WAIS: VIQ 91	Severe	None	Attention-deficit/hyperactivity disorder
Seizures	No	No	No	From age 14 years, severe	No	No	From birth, severe	No	No
Extracranial malformation		No	No	No	No	No	No	No	No
Hippocampal malformation	Yes				No	No	Yes		
Pituitary malformation	No	No			No	No			
Corpus callosum	Partial absence	Normal			No	Normal	Normal		
Hydrocephalus	No	No				No	Reported, not obvious in MRI		
Periventricular leukomalacia	No	No				No	Reported, not obvious in MRI		
Other features	Delayed speech, few words; left retinal detachment	Mother had previous stillbirth at 38 wk gestation	Mother had termination of pregnancy for brain malformation and microphthalmia; affected fetus (patient 3B[c]) carried the c.252delC mutation	Delayed speech, few words, later lost	Nystagmus	Anterior commissure thin; colliculi present, delayed speech and motor development		Bilateral retinal detachment, posterior vitreous opacities; unaffected brother has P133T mutation	Brachycephaly, dysplastic ears

NOTE.—Blank cells indicate that no information is available; WT = wild type; NA = not applicable (e.g., no cataracts when eye is anophthalmic); R = right; L = left.

[a] Patient 4C is the mildly affected mosaic mother of affected siblings 4A and 4B.

[b] Occipitofrontal circumference.

[c] Patient 3B (the affected fetus) and patient 3A are siblings; both carry the same mutation as their unaffected mosaic mother.

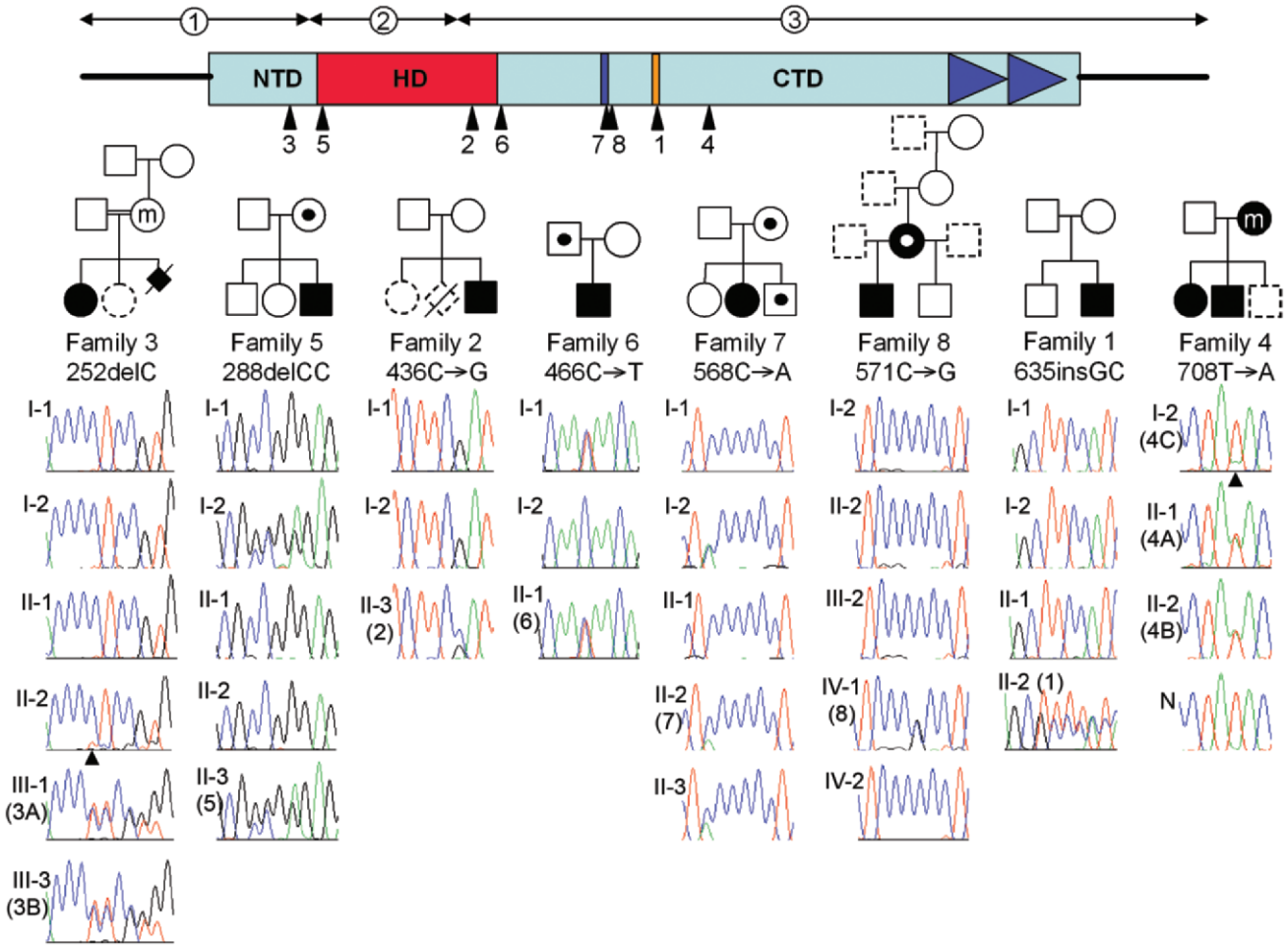

Figure 1 *OTX2* mutation analysis in eight families with congenital eye malformations. *Top,* Schematic diagram of the human *OTX2* cDNA, showing the homeodomain ("HD") (*red rectangle*); SIWSPA motif (*dark blue bar*); SGQFTP motif (*orange bar*); and tandemly repeated OTX-tail motif (*dark blue triangles*). NTD = N-terminal domain; CTD = C-terminal domain. Horizontal arrows show the extent of the three exons. Vertical arrowheads show the position of each mutation, with the corresponding family number. *Bottom,* Pedigrees with representative sequence traces. Genetic analysis was performed for all individuals except those with dashed outlines. Blackened symbol = affected; unblackened symbol = unaffected; dashed outline = individual not available for analysis; blackened dot in unblackened symbol = unaffected mutation carrier; unblackened dot in blackened symbol = affected individual without mutation; m = mosaic. Numbers to the left of each sequence trace indicate generation and individual; patient numbers are also shown (in parentheses). In family 3, individuals II-1 and II-2 are second cousins. For family 4, "N" is a normal control sequence for comparison. Arrowheads below the traces for individuals II-2 (family 3) and I-2 (family 4) indicate a low-level presence of the mutant allele.

ss35522250) and 269–70 C/A (dbSNP accession number ss35522251), and one already-known variant near the start of the 3′ UTR (c.1050 G/A) (dbSNP accession number rs171978).

MRI Data and Neuropsychometric Testing of OTX2 *Mutation Carriers*

Three of the patients with *OTX2* mutations have severe learning disabilities; these disabilities are associated, in two patients, with frequent seizures (table 2). These neurological phenotypes, together with the extensive expression of *OTX2* in the brain, indicated that MRI scans and neuropsychometric testing might be informative, as shown for *PAX6* (Sisodiya et al. 2001).

Patient 4B, patient 5, and the unaffected mother of patient 5 had MRI scans. Patient 5 and his mother also underwent neuropsychometric testing. Original diagnostic MRI data were reviewed for patients 1, 2, and 6, and CT data were reviewed for patient 3A. For patients 2 and 3A, only ocular data were available.

In four of the six patients for whom data are available, the optic nerves and optic chiasm are abnormal (fig. 3 and table 2). The nerves and chiasm are absent in patients 2 and 6 and are hypoplastic in patient 5. In patient 1, the optic nerve is absent on the anophthalmic

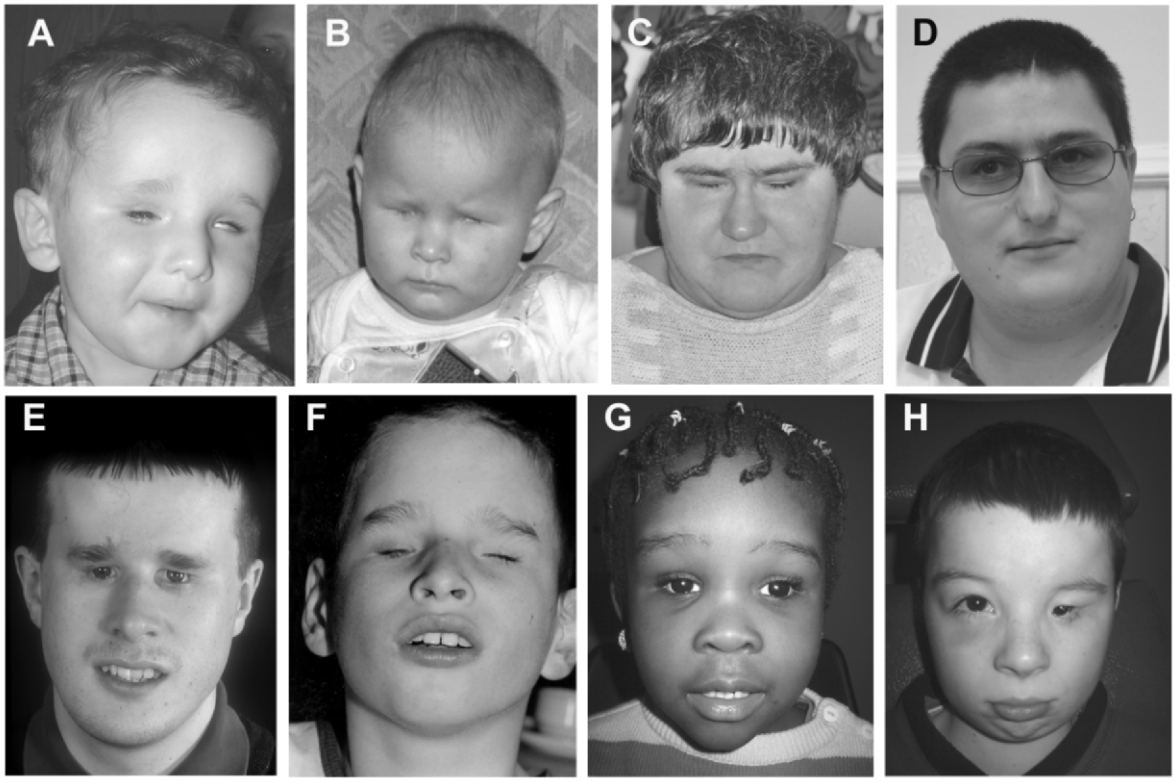

Figure 2 Facial views of eight patients with *OTX2* coding-region sequence changes: patient 1 (*A*), patient 3A (*B*), patient 4A (*C*), patient 4B (*D*), patient 5 (*E*), patient 6 (*F*), patient 7 (*G*), and patient 8 (*H*). Patients 5 and 7 are wearing prostheses in both eyes. Patient 8 is wearing a prosthesis in the left eye.

side and is hypoplastic on the microphthalmic side; the chiasm is thin.

Patients 3A and 5 both had slightly enlarged lateral ventricles. A striking cerebral anomaly is evident in patient 6, who has bilateral abnormal hippocampal morphology (fig. 5). A similar hippocampal malformation was seen, on review, in patient 1.

Patient 5 functions intellectually just within the average ability range (Wechsler Adult Intelligence Scale–Revised [WAIS-R]: verbal IQ [VIQ] 91). His verbal memory was good and was in keeping with his intellectual level (verbal learning and recall 25th–50th percentile). His performance on tests of executive skills was average. His 55-year-old mutation-carrying mother has no eye phenotype and functions intellectually at a level comparable to that found for her son (VIQ 96). Her memory was not as good as that of her son: after correcting for age, her scores were in the 10th–25th percentile. Executive skills were average.

Patient 2 was described as having cognitive and language skills at least age-appropriate for a blind child when a neurodisability assessment was performed at age 4.5 years.

RNA In Situ Hybridization

The developing human eye at CS16–CS19, like that of the mouse at a corresponding age, shows strong *OTX2* expression in the RPE layer and weaker *OTX2* expression in the neural retina (fig. 6*F*, 6*G*, and 6*H* and data not shown). Mice have low-level expression in the E11 neural retina, which becomes restricted to the neuroblastic layer by E17.5 and which remains present in the inner nuclear layer into the postnatal period (Martinez-Morales et al. 2001; Nishida et al. 2003).

OTX2 is widely expressed throughout the telencephalon and mesencephalon at CS14, with a sharp cutoff at the midbrain-hindbrain boundary (fig. 6*A*). *OTX2* expression was observed in the lamina terminalis and the floor of the telencephalon at CS16 (fig. 6*B* and 6*C*), sites that have also been reported in mouse (Simeone et al. 1993; Mallamaci et al. 1996; Simeone 2000). At CS22, *OTX2* was expressed in the choroid plexus, the dorsal thalamus, and the roof of the mesencephalon (fig. 6*E*). In the developing nasal structures, *OTX2* is seen in the olfactory epithelium of the nasal pits at CS18 (fig. 6*D*), again mirroring the mouse patterns.

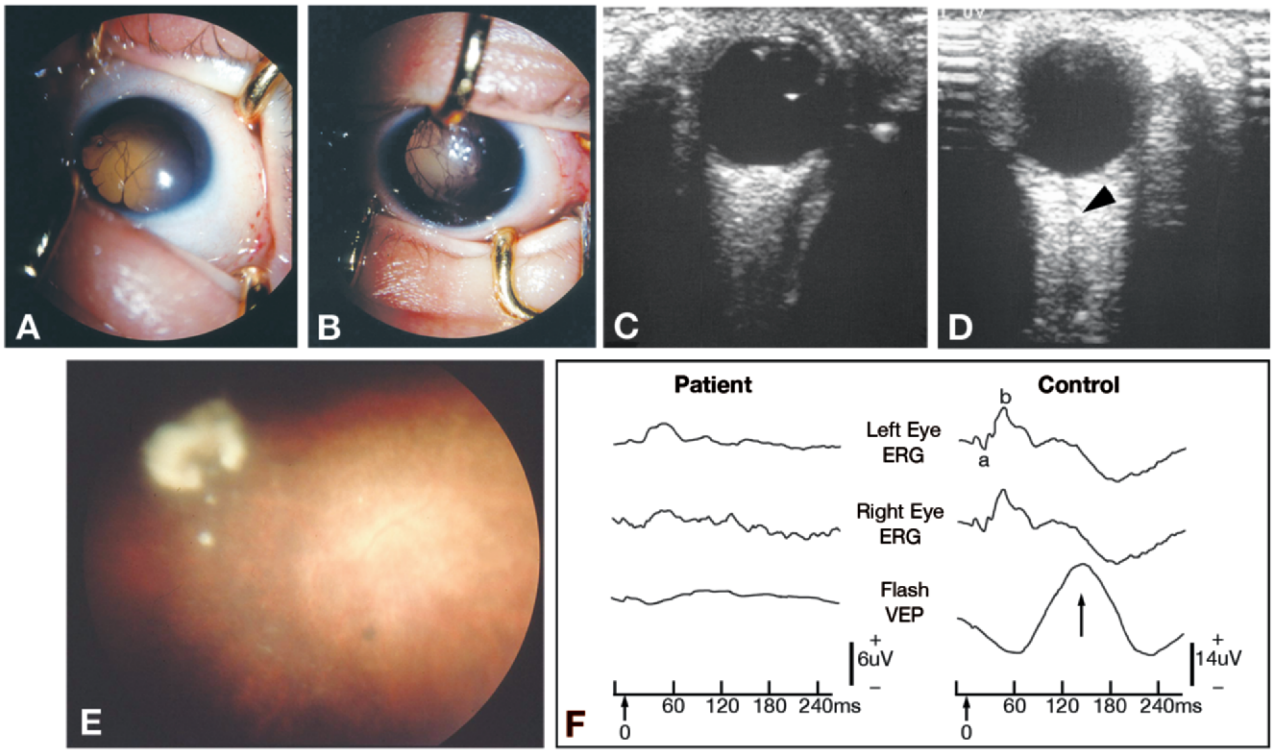

Figure 3 Ocular findings for patient 2 at age 6 wk. The right eye (*A*) and left eye (*B*) are shown, both with persistent pupillary membrane and tunica vasculosa lentis and a clear lens. Ultrasound scans of the right (*C*) and left (*D*) orbits show small eyes. In panel C, no optic nerve is visible. In panel D, the thin cord extending posteriorly from the globe (*arrowhead*) may be the optic-nerve sheath. The left fundus (*E*) has a white elevated area with a pigmented surrounding area and grayish tissue extending a short distance into the posterior segment. This may be a hyaloid remnant. No retinal vessels are visible. The fundus is hypopigmented, with a granular appearance and a few choroidal vessels. *F*, In electrophysiological tests, patient 2 (*left*) gave a small (<2 mV) but consistent response to flash "a" and "b" waves (control >10 mV). Visual evoked potential ("VEP") showed no consistent response to flash. Results from an age-matched control are shown (*right*).

Discussion

Using a candidate-gene approach, we found a wide spectrum of human phenotypes to be associated with *OTX2* coding-region sequence changes. The phenotypes were, however, significantly different from those in the mouse knockouts (Acampora et al. 1995; Matsuo et al. 1995; Ang et al. 1996). The inheritance patterns in the families are diverse.

Spectrum of OTX2 *Mutations and Genetic Mechanisms*

We found eight different heterozygous *OTX2* exonic changes in the patient cohort. Five of the eight changes are predicted to cause premature protein truncation either through direct creation of a stop codon or through a frameshift (fig. 1 and table 2). The only mutation predicted to lead to haploinsufficiency through nonsense-mediated decay (reviewed by Holbrook et al. [2004]) is in family 3, in which a stop codon is predicted in exon 2. In the other four families (1, 4, 5, and 6), termination is predicted in the last exon—making it likely that the truncated protein is expressed and that it may function in a dominant negative manner (Nussbaum et al. 2001).

The R89G de novo missense change found in patient 2 causes substitution of an invariant homeodomain arginine that is normally in contact with DNA phosphate residues. Missense mutations of the homologous residue have been identified in seven different homeodomain proteins, three of them (PITX2 [MIM 601542], SIX3 [MIM 603714], and CRX) associated with eye disease (Swaroop et al. 1999; D'Elia et al. 2001; Laflamme et al. 2004).

The mutations found in patient 1 (635insGC) and patient 2 (R89G) arose de novo. In siblings 3A and 3B (252delC) and siblings 4A and 4B (Y179X), the sequence changes were inherited from mothers who were found to carry, at a low level in blood DNA, the same mutation as their offspring. In both cases, the mother transmitted the mutation to two affected children, providing strong evidence that these mothers are gonosomal mosaics with a high frequency of mutant cells in their

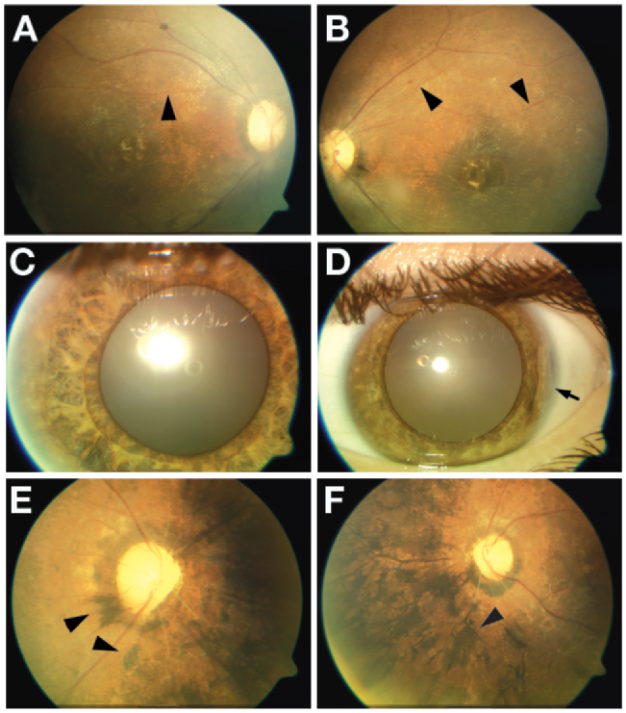

Figure 4 Ocular findings in family 4. Patient 4B at age 28 years: right fundus (*A*) and left fundus (*B*), both with pale optic disks, atrophic maculae, and thin retinal vessels (*arrowheads*); right iris (*C*) and left iris (*D*). The left iris has peripheral anterior synechiae (*arrow*). Patient 4C (mosaic mother of patients 4A and 4B) at age 51 years: right fundus (*E*) and left fundus (*F*), showing retinopathy with accumulated pigment clumps (*arrowheads*).

germ lines (Edwards 1989). The parents of the mosaic individual should not have the mutation, as observed in family 3 (fig. 1). Gonosomal mosaic individuals may or may not express clinical features themselves, depending on the proportion and distribution of mutant cells in their body. The mosaic mother in family 3 has undergone a full eye examination, including high-resolution multifocal electroretinogram (ERG), and is ophthalmologically normal. The mosaic mother in family 4 (patient 4C) has progressive retinal dystrophy (fig. 4*E* and 4*F*), with a self-reported history of undefined visual problems from an early age. Typically, an affected mosaic individual has a milder phenotype than his or her constitutive offspring (Zlotogora 1998). This seems to be true for patient 4C, since she has retinal pathology without the structural eye defects observed in her children.

Families 1–4 fit a model in which *OTX2* haploinsufficiency (loss of function in one allele) alone causes structural eye malformations. However, families 5 and 6 provide evidence of incomplete penetrance, since predicted protein-truncating mutations identified in bilateral anophthalmic children are also found in an unaffected mother and father, respectively (fig. 1 and table 2).

Results from families 7 and 8 are difficult to interpret. Both have missense substitutions at adjacent highly conserved proline residues, but the functional consequences of these sequence changes are unknown. Both families show discordance of phenotype and genotype. For family 7, no ethnically matched controls were available, so the frequency of the P133T change in the population of origin of family 7 is unknown. In family 8, the affected son has the P134A change, but his very similarly affected mother does not, making it highly unlikely that this sequence variant is a major contributor to the phenotype. We shall now focus on the loss-of-function mutations.

Two different models, based on recent insights from other human genetic diseases, may explain incomplete penetrance. First, if *OTX2* is the only locus involved, the level of gene expression may be affected by stochastic and/or genetic factors. This model assumes that an abnormal phenotype will be manifest if *OTX2* expression falls below a certain critical threshold level and if loss of function of one copy reduces gene expression levels close to this threshold. Stochastic fluctuations in transcription levels, possibly influenced by environmental factors but independent of genetic background, may reduce expression levels below the threshold. Evidence of this comes from the observation that genetically identical *Otx2*-knockout mice have highly variable phenotypes (Matsuo et al. 1995). Genetic factors at the mutant locus—specifically, regulatory polymorphisms of the normal allele—can also determine penetrance by controlling transcription levels (Gouya et al. 2002; Vithana et al. 2003). If the mutant allele is in *trans* to a strongly expressing normal allele, transcription is maintained above the threshold, which explains the clinically unaffected status of constitutive mutation carriers, but a weakly expressing normal allele leads to expression below the threshold required for normal development, and the abnormal phenotype is revealed (Gouya et al. 2002). The human *OTX2* locus spans >500 kb and has numerous distant enhancers that could be targets for regulatory polymorphisms (Kurokawa et al. 2004*b*).

Second, digenic or oligogenic inheritance may manifest as incomplete penetrance (Ming and Muenke 2002; van Heyningen and Yeyati 2004). An example of digenic inheritance is provided by a form of retinitis pigmentosa in which affected individuals have heterozygous mutations in both the *ROM1* (MIM 180721) and *RDS* (MIM 179605) genes, which encode related components of an oligomeric photoreceptor protein. Mutations at only one locus do not lead to an abnormal phenotype; penetrance is dependent on cosegregation of both mutations (Kajiwara et al. 1994). Perhaps more relevant to the developmental complexity of the eye and brain is holoprosencephaly (HPE [MIM 142945 and MIM 157170]), a disease that frequently shows non-Mendelian segregation patterns (Ming and Muenke 2002). The complex

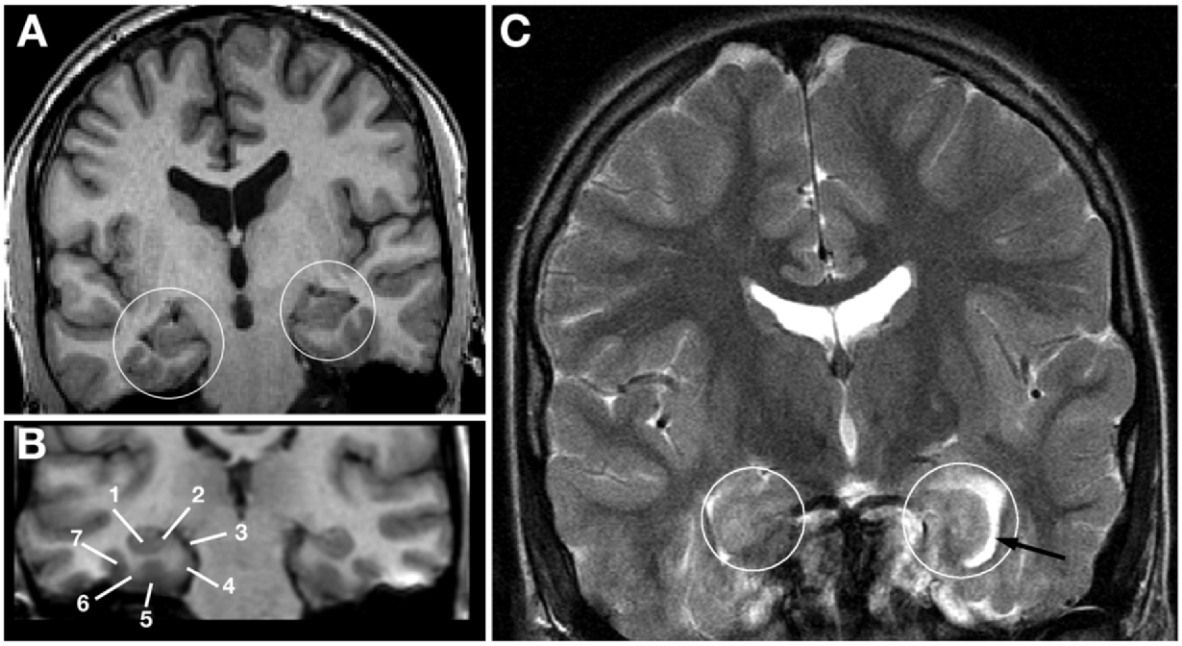

Figure 5 Coronal MRIs from patient 5 (T1-weighted image [*A*]), a normal control (T1-weighted image [*B*]), and patient 6 (T2-weighted image [C]). The left side of each image is the right side of the patient. In panels A and C, the hippocampi are circled. Panel B is labeled to show the normal hippocampal and parahippocampal structures: 1 = body of the hippocampus; 2 = subiculum; 3 = ambient cistern; 4 = parahippocampal gyrus; 5 = collateral sulcus; 6 = fusiform gyrus; 7 = lateral occipitotemporal sulcus. The hippocampi and parahippocampal structures are normal in panel A but are abnormal in panel C. Despite the different image parameters (T2 vs. T1 control), in panel C the hippocampi are more vertically aligned and are more globular than ovoid. Instead of being tucked laterally into the temporal horns of the lateral ventricles, the medial displacement and incomplete rotation of the hippocampi generate a cerebrospinal fluid–filled extension of the temporal horns of the lateral ventricle (*arrow*).

inheritance patterns and range of phenotypes we observe for *OTX2* are similar to those reported for *SHH* (MIM 600725) and *SIX3*, the major contributors toward HPE types 3 and 2, respectively (Nanni et al. 1999; Wallis et al. 1999). Whereas some HPE-associated *SHH* and *SIX3* mutations have arisen de novo, others have been inherited from completely unaffected carrier parents (Nanni et al. 1999; Wallis et al. 1999). The possibility that interaction with modifier gene variants at other loci may be required for full penetrance is supported by the observation that, in three reported cases, affected individuals carry mutations in two HPE genes (*SHH* with *TGIF* [MIM 602630] or *ZIC2* [MIM 603073]) (Nanni et al. 1999; Ming and Muenke 2002). Most HPE genes are involved in developmental signaling, and it is possible that reduction in the dosage of one protein can be buffered but two cannot, so that expression of an abnormal phenotype may depend on mutations in more than one gene (Ming and Muenke 2002).

Of six families with loss-of-function mutations, four have mutation-carrier parents (families 3, 4, 5, and 6 [fig. 1]), three of whom are unaffected. Two parents are probably constitutive mutation carriers, and two are gonosomal mosaics. This presents challenges for genetic counseling of families with *OTX2* mutations. Estimating the risk of having an affected child is extremely difficult. The relationship between levels of somatic and germline mosaicism is unpredictable. Little is known about either the precise stage at which the germ line is determined in humans or the number of precursor cells recruited. However, the number of cells ancestral to the germ line in mammals is thought to be small, so an individual who is gonosomal mosaic is likely to have a significant proportion of germ cells carrying the mutation (Zlotogora 1998; Leuer et al. 2001). Consequently, a relatively high recurrence risk is predicted for the offspring of gonosomal mosaic individuals, even if the proportion of mutant alleles in blood DNA is low. This has been observed in practice by others (Zlotogora 1998; Leuer et al. 2001) and in the present study, with both gonosomal mosaic mothers passing the mutation to two affected offspring. Constitutive-mutation-carrier parents are expected to be at 50% risk of having an affected child; however, recurrence was observed only in families with a mosaic parent. The lack of penetrance of *OTX2* mutations must also be taken into account; the recurrence risk will presumably be lower if, as we suggest, other factors are required for manifestation of an abnormal phenotype.

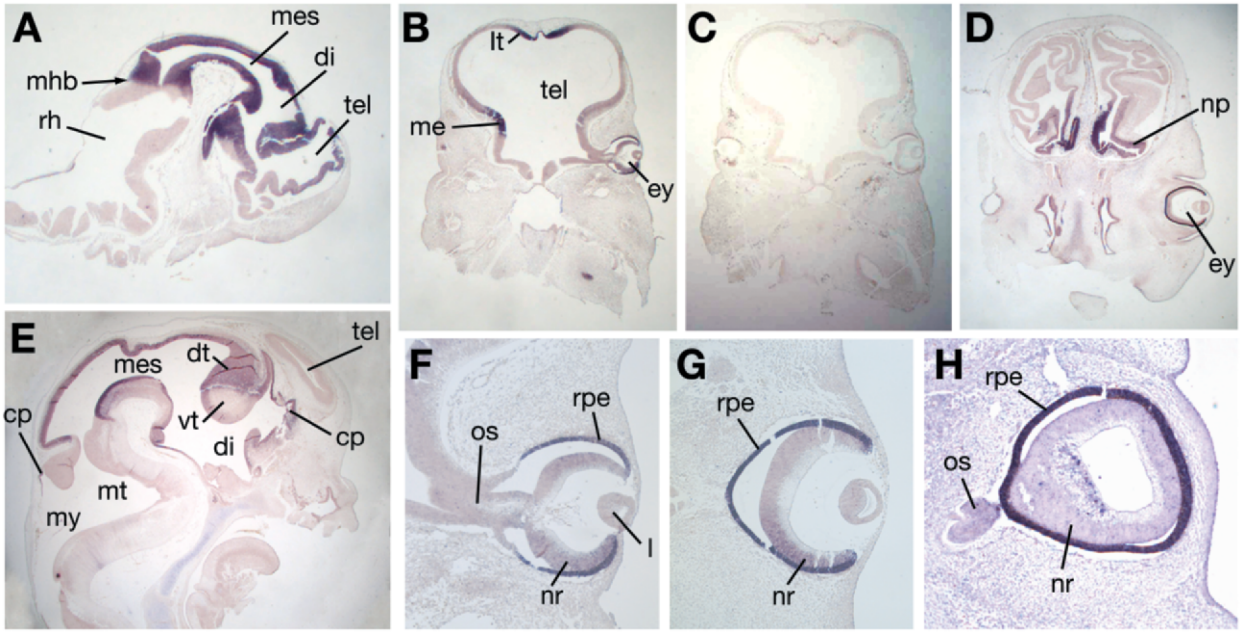

Figure 6 Expression pattern of the human *OTX2* gene in the developing head (*A–E*) and eye (*F–H*). Panels show representative results of nonradioactive in situ hybridization with a human *OTX2* probe. All panels (apart from panel *C*, which shows a sense control) show antisense hybridization: CS14 sagittal (*A*); CS16 coronal (*B* and *C*); CS18 (*D*); CS22 sagittal (*E*); CS16 5 × magnification of panel B (*F*); CS17 coronal (*G*); CS19 transverse (*H*). Strong expression is seen in the RPE (*panels B, D, F, G,* and *H*), and weaker expression is seen in the neural retina. Pigment formation has not yet begun at this stage; cp = choroid plexus; di = diencephalic vesicle; dt = dorsal thalamus; ey = eye; l = lens; lt = lamina terminalis; me = medial eminence; mes = mesencephalic vesicle; mhb = midbrain/hindbrain boundary; mt = metencephalic vesicle; my = myelencephalic vesicle; np = nasal pit; nr = neural retina; os = optic stalk; rh = rhombencephalic vesicle; rpe = retinal pigment epithelium; tel = telencephalic vesicle; vt = ventral thalamus.

The relevant factors are, however, already present in families with one or more affected offspring.

Unaffected parents may be constitutive or mosaic mutation carriers; therefore, it is essential to test them for any *OTX2* mutation identified in affected probands. However, accurate estimates of the recurrence risk await a molecular definition of the factors that determine penetrance of these mutations.

Phenotypic Variability

OTX2 loss-of-function mutations are associated with a broad spectrum of ocular phenotypes, ranging from bilateral anophthalmia to mild microphthalmia with retinal abnormalities. Asymmetry between the two sides, also noted in other genetic ocular malformations (Fantes et al. 2003; Ragge et al. 2005), is frequently seen. The spectrum of neurological phenotypes is broad, ranging from severe developmental delay to normal cognitive development. Variable expressivity is illustrated by the different phenotypes of siblings 4A and 4B.

The *OTX2* transcription pattern in human embryos is very similar to that described for mouse at the stages examined. This is not always the case (Fougerousse et al. 2000). The highly conserved expression pattern indicates conserved transcriptional control mechanisms. Analysis of the *Otx2* loci in human, mouse, *Xenopus,* zebrafish, and *Fugu* demonstrated that many of the distant enhancers that control *Otx2* expression are functionally conserved (Kurokawa et al. 2004*a*, 2004*b*). These elements, spread over hundreds of kilobases of genomic DNA, are possible targets for mutations/variations that might influence phenotypic severity and penetrance.

The ocular expression pattern of *OTX2* correlates well with the range of eye phenotypes observed in patients with loss-of-function mutations. *Otx2* interacts with *Mitf* to specify the RPE, which is essential for normal eye development (Martinez-Morales et al. 2003). Early RPE defects cause gross structural abnormalities of the eye (Raymond and Jackson 1995; Graw 2003). The anophthalmia and severe microphthalmia phenotypes in our cohort may result directly from loss of *OTX2* function in the developing RPE.

In the developing neural retina, OTX2 regulates *CRX,* and *CRX* mutations cause LCA and retinal degeneration (Sohocki et al. 1998; Rivolta et al. 2001; Nishida et al. 2003). The retinal phenotypes in patients 4B (with an original diagnosis of LCA) and 4C (resembling pigmen-

tary retinopathy) may be due to disturbed OTX2 regulation of CRX function.

The optic nerve and chiasm were reduced or absent in four of the six patients for whom MRI, CT, or ultrasound data were available (patients 1, 2, 5 and 6 [fig. 3 and table 2]). Optic-nerve aplasia, which is very rare, was observed bilaterally in patients 2 and 6, with absence of the chiasm, and unilaterally on the anophthalmic side in patient 1, who also shows a thin chiasm. Hypoplasia of optic nerves and chiasm was observed in patient 5. Although *OTX2*/*Otx2* is expressed in the optic stalk and subsequently in the optic-nerve sheath, it is not expressed in the optic nerve itself (fig. 6) (Simeone et al. 1993; Bovolenta et al. 1997; Martinez-Morales et al. 2001). Hypoplasia of the optic nerve and chiasm may therefore be a secondary effect of abnormal retinal development. The optic nerve is formed when retinal ganglion-cell axons exit the globe. The majority of axons, encased in the optic sheath, project to the contralateral side of the brain, forming the optic chiasm in the ventral diencephalon (Rasband et al. 2003). *Otx2* is expressed in retinal ganglion cells (Bovolenta et al. 1997), so *OTX2* mutations may compromise the development of the optic nerve and the formation of the chiasm.

Pronounced hippocampal malformation was observed (fig. 5*C*) in patient 6, with bilateral anophthalmia, severe developmental delay, and seizures beginning in infancy. The hippocampus is derived from the alar plate, which develops from an OTX2-expressing domain of the neural plate (Fernandez-Garre et al. 2002). Patient 4A was the other individual in the cohort with severe developmental delay and seizures with teenage onset (table 2). Unfortunately, no MRI information is available for this patient. However, a hippocampal abnormality similar to that in patient 6 was observed in patient 1, a young child with severe developmental and speech delay, like patient 4B, but currently without seizures. The association of hippocampal malformation with seizures remains to be confirmed as additional patients are identified.

It is interesting to note that the ocular defects reported in heterozygous *Otx2*-knockout mice were usually accompanied by severe craniofacial malformations (Matsuo et al. 1995). Our data show that heterozygous *OTX2* mutations in humans are associated with structural eye malformations in the absence of gross craniofacial abnormalities. However, the phenotypic composition of our study cohort leads to biased ascertainment of *OTX2* mutations in ocular malformation cases. A broader human mutation study might reveal *OTX2* mutations associated with craniofacial malformation syndromes or seizure-associated brain defects in the absence of eye anomalies.

We have presented evidence that heterozygous loss-of-function mutations in the *OTX2* gene make a major contribution to the genetic basis of anophthalmia and microphthalmia in a small but significant proportion of patients. Two notable findings of our study are the lack of penetrance of *OTX2* mutations and the high incidence of gonosomal mosaicism. The factors that influence de novo mutagenesis in the early embryo are unknown; it is unclear at present whether some genes or genomic regions are more susceptible than others following fertilization or whether gonosomal mosaicism is more common than previously recognized and has simply been underascertained. Of five nucleotide substitutions in our cohort, four are transversions and one is a transition: this unusual bias (Nachman and Crowell 2000) may hint at novel mutational mechanisms. Elucidation of the factors that influence *OTX2* penetrance is a high priority and will assist with genetic counseling; in addition, further studies will help to unravel the complex genetic interactions that are responsible for the development of the human eye.

Acknowledgments

We gratefully acknowledge the cooperation of the patients and their families. We thank Marie Restori of Moorfields Eye Hospital, for performing ocular ultrasound; Alison Condie of the Wellcome Trust Clinical Research Facility, Edinburgh, for technical assistance; John Stevens, for expert neuroradiology; and the Medical Research Council/Wellcome Trust–funded Human Developmental Biology Resource. N.K.R. is a Senior Surgical Scientist and is supported by the Academy of Medical Sciences/The Health Foundation and the Medical Research Fund, Oxford. I.M.H. is supported by a Career Development Award from the U.K. Medical Research Council.

Electronic-Database Information

Accession numbers and URLs for data presented herein are as follows:

dbSNP, http://www.ncbi.nlm.nih.gov/SNP/ (for 268+12 C/T [accession number ss35522250], 269–70 C/A [accession number ss35522251], and c.1050 G/A [accession number rs171978])

GenBank, http://www.ncbi.nlm.nih.gov/Genbank/ (for human *OTX2* cDNA [accession number NM_172337] and BAC AL161757)

Laboratory of Phil Green, http://www.phrap.org/index.html

Online Mendelian Inheritance in Man (OMIM), http://www.ncbi.nlm.nih.gov/Omim/ (for anophthalmia, extreme microphthalmia, sclerocornea, aniridia, colobomata, congenital cataracts, LCA, Walker-Warburg syndrome, congenital cataract/aphakia, *PAX6, RAX, CHX10, MAF, SOX2, OTX2, CRX,* cone-rod dystrophy, MITF, OTX1, optic-nerve aplasia, PITX2, SIX3, *ROM1, RDS,* HPE, *SHH, TGIF,* and *ZIC2)*

References

Acampora D, Mazan S, Lallemand Y, Avantaggiato V, Maury M, Simeone A, Brulet P (1995) Forebrain and midbrain

regions are deleted in $Otx2^{-/-}$ mutants due to a defective anterior neuroectoderm specification during gastrulation. Development 121:3279–3290

Aijaz S, Clark BJ, Williamson K, van Heyningen V, Morrison D, Fitzpatrick D, Collin R, Ragge N, Christoforou A, Brown A, Hanson I (2004) Absence of SIX6 mutations in microphthalmia, anophthalmia, and coloboma. Invest Ophthalmol Vis Sci 45:3871–3876

Ang SL, Jin O, Rhinn M, Daigle N, Stevenson L, Rossant J (1996) A targeted mouse Otx2 mutation leads to severe defects in gastrulation and formation of axial mesoderm and to deletion of rostral brain. Development 122:243–252

Azuma N, Yamaguchi Y, Handa H, Hayakawa M, Kanai A, Yamada M (1999) Missense mutation in the alternative splice region of the PAX6 gene in eye anomalies. Am J Hum Genet 65:656–663

Bovolenta P, Mallamaci A, Briata P, Corte G, Boncinelli E (1997) Implication of OTX2 in pigment epithelium determination and neural retina differentiation. J Neurosci 17: 4243–4252

Brewer C, Holloway S, Zawalnyski P, Schinzel A, FitzPatrick D (1998) A chromosomal deletion map of human malformations. Am J Hum Genet 63:1153–1159

D'Elia AV, Tell G, Paron I, Pellizzari L, Lonigro R, Damante G (2001) Missense mutations of human homeoboxes: a review. Hum Mutat 18:361–374

Dobyns WB, Pagon RA, Armstrong D, Curry CJ, Greenberg F, Grix A, Holmes LB, Laxova R, Michels VV, Robinow M, Zimmerman RL (1989) Diagnostic criteria for Walker-Warburg syndrome. Am J Med Genet 32:195–210

Edwards JH (1989) Familiarity, recessivity and germline mosaicism. Ann Hum Genet 53:33–47

Fantes J, Ragge NK, Lynch SA, McGill NI, Collin JR, Howard-Peebles PN, Hayward C, Vivian AJ, Williamson K, van Heyningen V, FitzPatrick DR (2003) Mutations in SOX2 cause anophthalmia. Nat Genet 33:461–463

Ferda-Percin E, Ploder LA, Yu JJ, Arici K, Horsford DJ, Rutherford A, Bapat B, Cox DW, Duncan AMV, Kalnins VI, Kocak-Altintas A, Sowden JC, Trabousli E, Sarfarazi M, McInnes RR (2000) Human microphthalmia associated with mutations in the retinal homeobox gene CHX10. Nat Genet 25:397–401

Fernandez-Garre P, Rodriguez-Gallardo L, Gallego-Diaz V, Alvarez IS, Puelles L (2002) Fate map of the chicken neural plate at stage 4. Development 129:2807–2822

Finkelstein R, Boncinelli E (1994) From fly head to mammalian forebrain: the story of otd and Otx. Trends Genet 10:310–315

Fledelius HC, Christensen AC (1996) Reappraisal of the human ocular growth curve in fetal life, infancy, and early childhood. Br J Ophthalmol 80:918–921

Fougerousse F, Bullen P, Herasse M, Lindsay S, Richard I, Wilson D, Suel L, Durand M, Robson S, Abitbol M, Beckmann JS, Strachan T (2000) Human-mouse differences in the embryonic expression patterns of developmental control genes and disease genes. Hum Mol Genet 9:165–173

Freund CL, Gregory-Evans CY, Furukawa T, Papaioannou M, Looser J, Ploder L, Bellingham J, Ng D, Herbrick JA, Duncan A, Scherer SW, Tsui LC, Loutradis-Anagnostou A, Jacobson SG, Cepko CL, Bhattacharya SS, McInnes RR (1997) Cone-rod dystrophy due to mutations in a novel photoreceptor-specific homeobox gene (CRX) essential for maintenance of the photoreceptor. Cell 91:543–553

Germot A, Lecointre G, Plouhinec JL, Le Mentec C, Girardot F, Mazan S (2001) Structural evolution of Otx genes in craniates. Mol Biol Evol 18:1668–1678

Gouya L, Puy H, Robreau AM, Bourgeois M, Lamoril J, Da Silva V, Grandchamp B, Deybach JC (2002) The penetrance of dominant erythropoietic protoporphyria is modulated by expression of wildtype FECH. Nat Genet 30:27–28

Graw J (2003) The genetic and molecular basis of congenital eye defects. Nat Rev Genet 4:876–888

Hanson I (2003) PAX6 and congenital eye malformations. Pediatr Res 54:791–796

Holbrook JA, Neu-Yilik G, Hentze MW, Kulozik AE (2004) Nonsense-mediated decay approaches the clinic. Nat Genet 36:801–808

Jamieson RV, Perveen R, Kerr B, Carette M, Yardley J, Heon E, Wirth MG, van Heyningen V, Donnai D, Munier F, Black GC (2002) Domain disruption and mutation of the bZIP transcription factor, MAF, associated with cataract, ocular anterior segment dysgenesis and coloboma. Hum Mol Genet 11:33–42

Kajiwara K, Berson EL, Dryja TP (1994) Digenic retinitis pigmentosa due to mutations at the unlinked peripherin/RDS and ROM1 loci. Science 264:1604–1608

Kurokawa D, Kiyonari H, Nakayama R, Kimura-Yoshida C, Matsuo I, Aizawa S (2004*a*) Regulation of Otx2 expression and its functions in mouse forebrain and midbrain. Development 131:3319–3331

Kurokawa D, Takasaki N, Kiyonari H, Nakayama R, Kimura-Yoshida C, Matsuo I, Aizawa S (2004*b*) Regulation of Otx2 expression and its functions in mouse epiblast and anterior neuroectoderm. Development 131:3307–3317

Laflamme C, Filion C, Labelle Y (2004) Functional characterization of SIX3 homeodomain mutations in holoprosencephaly: interaction with the nuclear receptor NR4A3/NOR1. Hum Mutat 24:502–508

Lai CSL, Gerrelli D, Monaco AP, Fisher SE, Copp AJ (2003) FOXP2 expression during brain development coincides with adult sites of pathology in a severe speech and language disorder. Brain 126:2455–2462

Leuer M, Oldenburg J, Lavergne JM, Ludwig M, Fregin A, Eigel A, Ljung R, Goodeve A, Peake I, Olek K (2001) Somatic mosaicism in hemophilia A: a fairly common event. Am J Hum Genet 69:75–87

Mallamaci A, Di Blas E, Briata P, Boncinelli E, Corte G (1996) OTX2 homeoprotein in the developing central nervous system and migratory cells of the olfactory area. Mech Dev 58: 165–178

Martinez-Morales JR, Dolez V, Rodrigo I, Zaccarini R, Leconte L, Bovolenta P, Saule S (2003) OTX2 activates the molecular network underlying retina pigment epithelium differentiation. J Biol Chem 278:21721–21731

Martinez-Morales JR, Signore M, Acampora D, Simeone A, Bovolenta P (2001) Otx genes are required for tissue specification in the developing eye. Development 128:2019–2030

Matsuo I, Kuratani S, Kimura C, Takeda N, Aizawa S (1995) Mouse Otx2 functions in the formation and patterning of the rostral head. Genes Dev 9:2646–2658

Ming JE, Muenke M (2002) Multiple hits during early embryonic development: digenic diseases and holoprosencephaly. Am J Hum Genet 71:1017–1032

Morrison D, FitzPatrick D, Hanson I, Williamson K, van Heyningen V, Fleck B, Jones I, Chalmers J, Campbell H (2002) National study of microphthalmia, anophthalmia, and coloboma (MAC) in Scotland: investigation of genetic aetiology. J Med Genet 39:16–22

Nachman MW, Crowell SL (2000) Estimate of the mutation rate per nucleotide in humans. Genetics 156:297–304

Nanni L, Ming JE, Bocian M, Steinhaus K, Bianchi DW, Die-Smulders C, Giannotti A, Imaizumi K, Jones KL, Campo MD, Martin RA, Meinecke P, Pierpont ME, Robin NH, Young ID, Roessler E, Muenke M (1999) The mutational spectrum of the sonic hedgehog gene in holoprosencephaly: SHH mutations cause a significant proportion of autosomal dominant holoprosencephaly. Hum Mol Genet 8:2479–2488

Nishida A, Furukawa A, Koike C, Tano Y, Aizawa S, Matsuo I, Furukawa T (2003) Otx2 homeobox gene controls retinal photoreceptor cell fate and pineal gland development. Nat Neurosci 6:1255–1263

Nussbaum RL, McInnes RR, Willard HF (2001) Genetics in medicine, 6th ed. W.B. Saunders, Philadelphia, p 54

Ragge NK, Lorenz B, Schneider A, Bushby K, de Sanctis L, de Sanctis U, Salt A, Collin JRO, Vivian AJ, Free SL, Thompson P, Williamson K, Sisodiya SM, van Heyningen V, Fitz-Patrick DR (2005) SOX2 anophthalmia syndrome. Am J Med Genet. http://www3.interscience.wiley.com/cgi-bin/fulltext/110437025/HTMLSTART/ (electronically published April 5, 2005; accessed April 20, 2005)

Rasband K, Hardy M, Chien C-B (2003) Generating X: formation of the optic chiasm. Neuron 39:885–888

Raymond SM, Jackson IJ (1995) The retinal pigmented epithelium is required for development and maintenance of the mouse neural retina. Curr Biol 5:1286–1295

Rivolta C, Berson EL, Dryja TP (2001) Dominant Leber congenital amaurosis, cone-rod degeneration, and retinitis pigmentosa caused by mutant versions of the transcription factor CRX. Hum Mutat 18:488–498

Simeone A (2000) Positioning the isthmic organizer where Otx2 and Gbx2 meet. Trends Genet 16:237–240

Simeone A, Acampora D, Mallamaci A, Stornaiuolo A, D'Apice MR, Nigro V, Boncinelli E (1993) A vertebrate gene related to orthodenticle contains a homeodomain of the bicoid class and demarcates anterior neuroectoderm in the gastrulating mouse embryo. EMBO J 12:2735–2747

Sisodiya SM, Free SL, Williamson KA, Mitchell TN, Willis C, Stevens JM, Kendall BE, Shorvon SD, Hanson IM, Moore AT, van Heyningen V (2001) PAX6 haploinsufficiency causes cerebral malformation and olfactory dysfunction in humans. Nat Genet 28:214–216

Sohocki MM, Sullivan LS, Mintz-Hittner HA, Birch D, Heckenlively JR, Freund CL, McInnes RR, Daiger SP (1998) A range of clinical phenotypes associated with mutations in *CRX,* a photoreceptor transcription-factor gene. Am J Hum Genet 63:1307–1315

Swaroop A, Wang QL, Wu W, Cook J, Coats C, Xu S, Chen S, Zack DJ, Sieving P (1999) Leber congenital amaurosis caused by a homozygous mutation (R90W) in the homeodomain of the retinal transcription factor CRX: direct evidence for the involvement of CRX in the development of photoreceptor function. Hum Mol Genet 8:299–305

Tahayato A, Sonneville R, Pichaud F, Wernet MF, Papatsenko D, Beaufils P, Cook T, Desplan C (2003) Otd/Crx, a dual regulator for the specification of ommatidia subtypes in the *Drosophila* retina. Dev Cell 5:391–402

van Heyningen V, Yeyati PL (2004) Mechanisms of non-Mendelian inheritance in genetic disease. Hum Mol Genet 13 Spec No 2:R225–R233

Vithana EN, Abu-Safieh L, Pelosini L, Winchester E, Hornan D, Bird AC, Hunt DM, Bustin SA, Bhattacharya SS (2003) Expression of PRPF31 mRNA in patients with autosomal dominant retinitis pigmentosa: a molecular clue for incomplete penetrance? Invest Ophthalmol Vis Sci 44:4204–4209

Voronina VA, Kozhemyakina EA, O'Kernick CM, Kahn ND, Wenger SL, Linberg JV, Schneider AS, Mathers PH (2004) Mutation in the human RAX homeobox gene in a patient with anophthalmia and sclerocornea. Hum Mol Genet 13: 315–322

Wallis DE, Roessler E, Hehr U, Nanni L, Wiltshire T, Richieri-Costa A, Gillessen-Kaesbach G, Zackai EH, Rommens J, Muenke M (1999) Mutations in the homeodomain of the human SIX3 gene cause holoprosencephaly. Nat Genet 22: 196–198

Zlotogora J (1998) Germ line mosaicism. Hum Genet 102: 381–386

Zuber ME, Gestri G, Viczian AS, Barsacchi G, Harris WA (2003) Specification of the vertebrate eye by a network of eye field transcription factors. Development 130:5155–5167